International Immunology, Vol. 22, No. 8, pp. 637–649
doi:10.1093/intimm/dxq048
Advance Access publication 25 May 2010

MT6-MMP is present in lipid rafts and faces inward in living human PMNs but translocates to the cell surface during neutrophil apoptosis

Carl F. Fortin[1], Anjum Sohail[2], Qing Sun[2], Patrick P. McDonald[1], Rafael Fridman[2] and **Tamàs Fülöp[3]**

[1]Faculty of Medicine and Health Sciences, Université de Sherbrooke, Sherbrooke, Québec J1H 5N4, Canada.
[2]Department of Pathology and Karmanos Cancer Institute, Wayne State University, Detroit, Michigan 48202, USA.
[3]Biogerontology Laboratory, Department of Medicine, Centre de Recherche sur le Vieillissement, Institut Universitaire de Gériatrie de Sherbrooke, Université de Sherbrooke, 375 Rue Argyll, Sherbrooke, Québec J1J 3H5, Canada.

Correspondence to: T. Fulop; E-mail: tamas.fulop@usherbrooke.ca

Transmitting editor: A. Falus

Received 29 January 2010, *accepted* 15 April 2010

Abstract

Polymorphonuclear neutrophils (PMNs) are the first line of defense against invading organisms in humans; in addition, PMNs contribute to the linking of innate and adaptive immunity. To fulfill their biological behavior, PMNs utilize an arsenal of proteolytic enzymes, including members of the matrix metalloproteinase family of zinc-dependent endopeptidases. PMNs express high levels of MT6-MMP (MMP-25), a glycosyl-phosphatidylinositol-anchored MMP, that belongs to the subfamily of membrane-anchored matrix metalloproteinases. Due to the paucity of information on MT6-MMP in primary cells, we set to investigate the localization and potential function of MT6-MMP in human PMNs. We found that MT6-MMP is present in the membrane, granules and nuclear/endoplasmic reticulum/Golgi fractions of PMNs where it is displayed as a disulfide-linked homodimer of 120 kDa. Stimulation of PMNs resulted in secretion of active MT6-MMP into the supernatants. Membrane-bound MT6-MMP, conversely, is located in the lipid rafts of resting PMNs and stimulation does not alter this location. In addition, TIMP-2, a natural inhibitor of MT6-MMP, does not co-localize with it in the lipid rafts. Interestingly, living PMNs do not display MT6-MMP on the cell surface. However, induction of apoptosis induces MT6-MMP relocation on PMNs' cell surface. Our studies suggest that metalloproteinases may play a role in respiratory burst and IL-8 secretion, but not chemotaxis or granulocyte macrophage colony-stimulating factor-induced survival. Collectively, these results provide new insights on the role of MT6-MMP in the physiology of human PMNs.

Keywords: apoptosis, chemotaxis, cytokines, lipid rafts, matrix metalloproteinase, neutrophils

Introduction

Polymorphonuclear neutrophils (PMNs) are circulating white blood cells that are major mediators of the innate immune system. PMNs are recruited from the circulation to the sites of infection and are the first cells in contact with potential invading pathogens. Upon their recruitment to the site of aggression, PMNs attempt to clear it from invading cells, microbes or debris by phagocytosis. If the site is successfully cleared of dangers, PMNs are removed from the site by apoptosis, a critical process leading to the resolution of inflammation (1, 2). The failure to appropriately remove PMNs from cleared site of inflammation is potentially detrimental, leading, for example to chronic inflammation (3). However, PMNs are much more than terminally differentiated phagocytes with an unforgiving appetite (4). Indeed, activated PMNs release cytokines and chemokines that profoundly influence the development of the subsequent immune response (5–7). In addition, PMNs release an impressive array of proteolytic enzymes that are used for PMNs' anti-pathogen functions (8).

Among the families of proteases produced by PMNs, the matrix metalloproteinase family constitutes a major group. PMNs produce three major metalloproteinases: MMP-9 (gelatinase B) (9); MMP-8 (neutrophil collagenase) (10) and MT6-MMP (MMP-25, leukolysin) (11, 12). While there is ample information on the expression and function of MMP-9 and MMP-8 in PMNs, there is only limited data on MT6-MMP (11). MT6-MMP belongs to the subfamily of membrane-anchored matrix metalloproteinases, named membrane-type

matrix metalloproteinase (MT-MMP), whose members are tethered to cell membranes via a glycosyl-phosphatidylinositol (GPI) anchor (11–13). MT6-MMP is produced in a monomeric latent form of ~57–60 kDa, which generates disulfide-bonded homodimers via a cysteine residue present in the stem region (13). Studies using recombinant MT6-MMP showed that the zymogen homodimer undergoes activation in the trans-Golgi network, likely by cleavage of the pro-peptide domain by a furin-mediated process, which is a common feature of the members of the MT-MMP family. Once activated, the MT6-MMP is displayed on the cell surface in a dimeric form of ~120 kDa (13, 14). It was previously shown that MT6-MMP is targeted to lipid rafts (13, 15), specialized membrane domains that have been implicated in signaling events and sorting of membrane proteins. However, MT6-MMP's precise function and substrates in lipid rafts remain unknown. Previous studies demonstrated that MT6-MMP is highly expressed in human PMNs (11) and in HL-60 cells induced to differentiate into PMN-like cells (14). In PMNs, the majority of MT6-MMP was localized in gelatinase granules while a minor fraction was detected in the cellular membrane (11). Exposure of human PMNs to phorbol ester [phorbol 12-myristate 13-acetate (PMA)] or IL-1α and IL-8 was found to induce the release of MT6-MMP from the granules into the extracellular space (11). Since this pioneering study of Kang *et al.* (11), there is only very few additional data on MT6-MMP localization and function in PMNs. Matsuda *et al.* (16) showed that, in PMNs, MT6-MMP can be found complexed with clusterin, and Nie and Pei (17) reported that MT6-MMP inactivated the alpha-1-proteinase inhibitor.

In consequence, the aim of the present study was to further investigate the expression and localization of MT6-MMP and its inhibitor TIMP-2 in primary human PMNs and to gain more detailed insights into its potential physiological functions. The studies presented herein provide novel information on the distribution of MT6-MMP in living and apoptotic PMNs and suggest that MT6-MMP contributes to some of PMN functions, such as respiratory burst and chemokine secretion.

Methods

Antibodies and reagents

Rabbit polyclonal antibodies against the hinge region (ab39034) of human MT6-MMP and against human TIMP-2 (ab53730) were from Abcam (Cambridge, MA, USA). Rabbit anti-flotillin-1 IgG (H-104) (sc-25506), goat anti-MT6-MMP IgG (C-13) (sc-20916), normal rabbit IgG (sc-2027), normal mouse IgG (sc-2025), anti-Annexin V (FL-319) (sc-8300), donkey anti-goat IgG (sc-2020) and rabbit anti-IκB-α (FL) (sc-371) were all from Santa Cruz Biotechnology (Santa Cruz, CA, USA). Mouse anti-human MT6-MMP mAb clone 141811 (MAB11422) was purchased from R&D Systems (Minneapolis, MN, USA). Anti-rabbit IgG coupled to Atto 647N fluorescent dye (40839), Protein A–Agarose (P9269), Protein G–Agarose (P7700) beads and poly-L-lysine solution were from Sigma–Aldrich (St Louis, MO, USA). Rabbit (NA934) or mouse (NA931) IgG (HRP-linked whole antibody) and Ficoll-Paque PLUS (17-1440-03) were from GE Healthcare Bio-sciences (Baie d'Urfé, Quebec, Canada). Triton X-100 and Nonidet P40 were from Roche (Laval, Quebec, Canada). DCFDA (carboxy-H2DCFDA) and cholera toxin coupled to AlexaFluor 488 (CT-488) were from Molecular Probes (Burlington, Ontario, Canada). Anti-human CD16 (555403) and anti-mouse IgG–FITC conjugate (554001) were from BD Biosciences (Mississauga, Ontario, Canada). Endotoxin-free RPMI 1640 media and fetal bovine serum (FBS) were from Wisent (St-Jean-Baptiste, Québec, Canada). PMA, diisopropyl fluorophosphates, formyl methionine-leucine-phenylalanine (fMLP), phenylmethylsulfonylfluoride (PMSF), pyrrolidine dithiocarbamate and LPS from *Escherichia coli* 0111:B4 were purchased from Sigma–Aldrich. Recombinant human cytokines were purchased from R&D Systems. All other reagents not mentioned here were purchased from Sigma–Aldrich.

PMN isolation and culture

Human PMNs were isolated from peripheral blood of healthy donors using a protocol approved by our Institutional Ethics Committee. All donors gave their informed written consent. The entire procedure was carried out at room temperature under endotoxin-free conditions using a modification of the method of Boyum *et al.* (18). Briefly, 450 ml of blood were collected by venipuncture and spun at 200 × *g* for 15 min and plasma was removed carefully and replaced with sterile PBS. Following sedimentation of erythrocytes with 0.5% dextran (final concentration) for 45 min, the cells were centrifuged over Ficoll-Paque cushions (400 × *g* for 20 min), and the resulting PBMC ring was carefully collected in new tubes. The remaining erythrocytes in the pellet were removed by a 20-s hypotonic lysis in water. After a wash with PBS, purified PMNs were spun at 210 × *g* for 10 min and suspended in RPMI 1640 supplemented with 5% autologous heat-denatured serum from the plasma of the blood donor (RPMI) at a concentration of 5×10^6 cells per ml for stimulation, unless otherwise stated. This procedure yields ~0.8 to 1.2×10^9 cells containing routinely 0.1% (but not >0.3%) contaminating monocytes or lymphocytes and <6% eosinophils. The purity of the PMN preparation was determined by Wright staining and by flow cytometry analysis of cellular granularity (side scatter). PMN viability exceeds 99% after culture for up to 6 h, as determined by trypan blue exclusion.

Subcellular fractionation of PMNs

To obtain the different cellular fractions of PMNs [membrane, cytoplasm, granules and a fraction containing the nucleus, the endoplasmic reticulum (ER) and the Golgi apparatus], a combination of nitrogen cavitation and centrifugation of the resulting cavitates was used, as already described (19). Briefly, PMNs (1×10^8) were disrupted by nitrogen cavitation in resting state or after stimulation with 100 U ml^{-1} of IL-1α in RPMI. Nuclear fractions were obtained by centrifugation of these cavitates at 2000 × *g* for 10 min at 4°C. Since this procedure does not remove contaminating ER or Golgi network, this fraction was named nucleus/ER. To obtain all granule subtypes, cavitates from the previous step were centrifuged at 20 000 × *g* for 10 min at 4°C. For membrane preparation [consisting of plasma membrane and

secretory vesicles (11)], the same cavitates (now free of nucleus/ER and granules) were ultracentrifuged (200 000 × *g* for 60 min at 4°C). After the ultracentrifugation, the remaining cavitates are free of organelles and contain only cytosolic proteins; hence, it is herein referred to as cytosolic fraction. All subcellular fractions were washed twice with cold PBS before being boiled in 2× sample buffer with or without the reducing agent (described below) and processed for immunoblot analysis. These different cellular fractions are exempt from mutual cross-contamination in these specific experimental settings, as already described (19).

Lipid raft preparation

PMNs (4×10^7 cells) were incubated with RPMI without or with 100 U ml^{-1} of IL-1α for 20 min at 37°C. The cells were then washed with cold PBS and re-suspended in 300 μl of ice-cold lipid raft lysis buffer (25 mM HEPES, pH 6.9, supplemented with 100 mM NaCl, 2 mM EDTA, 2 mM $NaVO_4$, 1 mM PMSF, 0.5% Triton, 10 μg ml^{-1} aprotinin and 10 μg ml^{-1} leupeptin). The lysates were cleared of cellular debris by centrifugation and dissolved in 300 μl of a cold sucrose solution (85% w/v in HEPES-buffered saline) to a final concentration of 42.5%. This solution was transferred to 2-ml ultracentrifuge tubes and gently overlaid with 1 ml of a 35% sucrose solution followed by 300 μl of a 5% sucrose solution. Centrifugations were carried out at 4°C for 16 h at 200 000 × *g* in a Beckman TLA-100.4 rotor (Beckman Instruments, Montreal, Quebec, Canada). Nine fractions of 200 μl each were collected from the top of the gradient and boiled in reducing or non-reducing 2× sample buffer for immunoblot analyses, as described below. Under these experimental conditions, lipid rafts are present in fractions 1–3 and non-lipid rafts are present in fractions 5–8, as described earlier (20).

Immunoblot analysis

For whole-cell lysates, PMNs (5×10^6 cells) were lysed in 100 μl of ice-cold PBS and 100 μl of reducing 2× sample buffer [50 mM Tris, pH 6.8, 4% sodium dodecyl sulfate (SDS) (w/v), 10% β-mercaptoethanol (β-ME, v/v) and 20% glycerol (v/v)] (21). The samples were boiled for 10 min, sonicated, snap frozen in liquid nitrogen and stored at −20°C until analysis. All samples were subjected to SDS–PAGE according to the method of Laemmli (22). Following SDS–PAGE, proteins were transferred onto nitrocellulose membranes and processed for immunoblot analysis as described previously (21). Samples resulting from subcellular fractionation procedures or lipid raft preparation were prepared by the addition of either reducing 2× sample buffer or by the addition of non-reducing 2× sample buffer (same as above, but with no β-ME) and resolved by SDS–PAGE followed by immunoblot analyses.

Confocal microscopy

PMNs were stimulated with 100 U ml^{-1} of IL-1α or RPMI for 20 min at 37°C, and stimulation was stopped by quick centrifugation and the cells were then fixed by 8% PFA in PBS for 15 min on ice. After permeabilization with 0.1% Triton X-100 in PBS for 10 min on ice, the cells were incubated with 10% rabbit serum for 30 min on ice. After a wash with PBS, the cells were incubated with primary antibodies (MT6-MMP hinge or isotype control) for 90 min on ice in PBS containing 1.5% rabbit serum and 0.1% Triton X-100. The PMNs were then washed twice with cold PBS and incubated with a secondary antibody (anti-rabbit-Atto 647) in the same conditions as for primary antibody but with addition of 1 μg of CT-488. After two washes with PBS, the cells were placed on poly-L-lysine-covered slides and mounted with VECTASHIELD Mounting Media (Vector Laboratories, Burlington, Ontario, Canada) and were examined with a scanning confocal microscope (FV1000, Olympus, Tokyo, Japan) coupled to an inverted microscope with a ×63 oil immersion objective (Olympus). Specimens were laser excited at 488 nm (40 mW argon laser) and 633 nm [helium–neon (red) laser]. A horizontal optical section of 512 × 512 pixels with two times line averaging was taken at one interval through the cell (optical resolution—lateral: 0.2 μm; axial: 0.8 μm). Images were acquired during the same day, typically from five fields from each experimental condition, using identical settings of the instrument. For Alexa 488/Atto 647 merged fluorescence images, dot fluorograms were obtained by plotting pixel values of each fluorochrome toward horizontal and vertical axis, respectively. Quadrant markers were placed to separate the staining in background pixels (C: low left), red-only pixels (A: up-left), green-only pixels (D: low right) and co-localizing pixels (B: up-right) and percentage of co-localization was assessed as follows: (# pixels in B)/(# pixels in B + # pixels in D). For illustration purposes, images were contrast-enhanced, pseudocolored according to their original fluorochromes, merged (co-localizing green and red pixels are yellow), cropped and then assembled using FluoView (Olympus) and Adobe Photoshop software (Adobe Systems, Mountain View, CA, USA).

Immunoprecipitation of released MT6-MMP

PMNs (2×10^7 cells per ml) were allowed to sediment for 55 min at 37°C in RPMI to promote cell–cell adherence (hereafter referred to as adherent PMNs). Adherent PMNs were then incubated with 4 nM PMA, 100 U IFN-γ, 100 U ml^{-1} IL-1α or 30 nM fMLP for 20 min at 37°C in RPMI. After the stimulation, the solutions were collected and centrifuged. The supernatants were collected and pre-cleared with 20 μl of protein A/G beads (50% slurry in PBS) for 30 min at 4°C. The mixtures were then centrifuged and the supernatants were collected and incubated with 1 μg of rabbit anti-MT6-MMP (hinge region) or non-immune rabbit IgG for 2 h at 4°C; this was followed by the addition of 35 μl protein A/G beads. After an overnight incubation at 4°C with end-over-end rotation, the beads were washed twice with PBS and processed for immunoblot analyses or enzymatic activity assays. For immunoblot analysis, the beads were boiled in 3× reducing sample buffer and the samples were resolved by SDS–PAGE followed by immunoblot analysis with an anti-human MT6-MMP antibody raised in goat. For the measurement of MT6-MMP enzymatic activity, the beads were washed again twice with cold assay buffer (described below) before substrate addition.

MT6-MMP catalytic activity assay

Enzymatic activity of immunoprecipitated MT6-MMP was monitored using the synthetic fluorescence-quenched peptide substrate (7-methoxycoumarin-4-yl) acetyl-L-prolyl-L-leucyl-L-glycyl-leucyl-(*N*3-(2,4-dinitrophenol)-L-2,3-diaminopropionyl)-L-alanyl-L-arginine amide (from Peptides International, Louisville, KY, USA) as described (13). Briefly, protein A/G beads containing bound MT6-MMP, as described above, were incubated with 20 μM of the substrate in assay buffer (50 mM HEPES, pH 7.5, 150 mM NaCl and 5 mM $CaCl_2$) with agitation at room temperature for 5 h in a final volume of 500 μl. The reaction mixtures were centrifuged (20 000 × *g*, 5 min) and the supernatants were collected. Hydrolysis of the fluorogenic substrate in the supernatants was monitored by a spectrofluorometer with excitation and emission wavelengths set at 328 and 393 nm, respectively. Controls included peptide substrate incubated with protein A/G beads and isotype antibody (rabbit IgG) or with whole-cell lysates of human PMNs (1.25×10^6 cells) prepared with lysis buffer (50 mM Tris, pH 7.5, supplemented with 1% Triton X-100, 150 mM NaCl, 10 mM EGTA and 5 mM EDTA). Results are shown as stimulation index: measured hydrolysis of the fluorogenic substrate of stimulated PMNs relative to the fluorescence of control media that contain no PMNs but only beads and rabbit IgG antibody.

Flow cytometry

Live PMNs (2.5×10^5 cells) were incubated with rabbit anti-MT6-MMP (hinge region), mouse anti-MT6-MMP (whole molecule) or isotype control antibodies (1 μg ml^{-1}) for 60 min on ice in PBS supplemented with 1% FBS and 1.5% rabbit serum. The cells were then washed twice with PBS and incubated on ice for an additional 60 min with FITC-coupled secondary antibodies (anti-rabbit– or anti-mouse–FITC) and 250 ng of propidium iodine (PI). The cells were washed and subjected to flow cytometry analysis (FACScalibur from Becton Dickinson, Franklin Lakes, NJ, USA) by gating on PI-excluded cells (to exclude damaged cells or cells in necrosis). As a positive control, PMNs were immunostained for CD16 (FcγRIII: low-affinity Fc receptor) with a mouse anti-CD16 antibody under the same conditions. As a negative control, PMNs were immunostained for IκB-α, a cytosolic protein, using a specific antibody. In a separate series of experiments, live, unfixed, PMNs (1×10^7 cells) were cultured at 37°C for 24 h in RPMI without or with 1 nM granulocyte macrophage colony-stimulating factor (GM-CSF). The cells were then processed for MT6-MMP immunostaining and PI staining, as described above. Expression of MT6-MMP at the cell surface was analyzed by acquiring 20 000 events on a FACScalibur instrument.

Measurement of respiratory burst by DCFDA cleavage

PMNs (1×10^6) in 500 μl PBS were loaded with 20 μM DCFDA at 37°C for 15 min and then stimulated with 4 nM PMA or 30 nM fMLP, as indicated. Fluorescence in the FL-1 channel was measured with a FACScalibur from Becton Dickinson, as described (21). For the experiments with *N*-acetyl-L-cysteine (NAC) or GM6001, PMNs were incubated for 30 min at 37°C with 20 mM NAC or 5 μM GM6001, loaded with DCFDA and stimulated as indicated. Data are shown as stimulation index representing mean fluorescence intensity (MFI) of stimulated cells relative to MFI of loaded, but resting, cells.

ELISA analysis of secreted IL-8

PMNs (3×10^6 cells in 600 μl) were cultured in 24-well culture plates at 37°C under a 5% CO_2 atmosphere in the presence or absence of 100 ng ml^{-1} LPS or 100 U ml^{-1} tumor necrosis factor (TNF)-α for 24 h in RPMI. Where indicated, 5 μM of GM6001 was added 30 min before stimulation. Culture supernatants were collected by centrifugation, snap frozen in liquid nitrogen and stored at −80°C until use. Cytokine concentrations (detection limits of this assay is 3 pg ml^{-1}) were determined with an in-house sandwich ELISA assays using commercially available capture and detection antibody pairs for IL-8 (BD PharMingen).

Statistical analysis

Statistical differences between groups were analyzed by unpaired *t*-tests using GraphPad Prism version 5.0c for Mac OS X, GraphPad software, San Diego, CA, USA, www.graphpad.com.

Results

Distribution of MT6-MMP and TIMP-2 in fractionated human PMNs

We first examined the cellular distribution of MT6-MMP in fractionated resting and IL-1α-stimulated PMNs. As shown in Fig. 1(A), MT6-MMP was detected in granules, membranes and nuclear/ER fractions, but not in the cytosol, in agreement with previous studies (11). Under reducing conditions (upper panels), MT6-MMP was detected as a major ~57-kDa form, representing the monomeric species, as described (13). In addition, under reducing conditions, a minor ~45-kDa immunoreactive form was mainly detected in the nuclear/ER fraction of IL-1α-stimulated PMNs (Fig. 1A, compare upper panels); possibly representing a degradation product and/or an underglycosylated precursor species of MT6-MMP, which is a glycoprotein (14). No significant differences in MT6-MMP distribution were found between resting and stimulated PMNs in samples analyzed under reducing conditions. Under non-reducing conditions (Fig. 1A, lower panels), resting PMNs contained the ~120-kDa dimeric form of MT6-MMP in the membranes and granules but not in the nucleus/ER, whereas in stimulated PMNs, MT6-MMP homodimers were found in all fractions except the cytosol. The differential presence of MT6-MMP in the nuclear/ER fraction between resting and stimulated PMNs may be due to homodimerization of MT6-MMP in response to IL-1α.

Since TIMP-1 and TIMP-2 inhibit MT6-MMP activity (13, 14, 16, 23, 24), we studied their localization in subcellular fractions of resting and stimulated PMNs. TIMP-1 was not detected in any of the fractions (data not shown), consistent with a lack of detectable TIMP-1 in human PMNs, as previously reported (25, 26). In contrast, TIMP-2 (~22 kDa) was readily detected in the granules (Fig. 1B, upper panel) and in the nuclear/ER/Golgi fraction (Fig. 1B, upper panel). TIMP-2 was, however, undetectable in the cytosol and in the membranes even after IL-1α stimulation (Fig. 1B). Upon

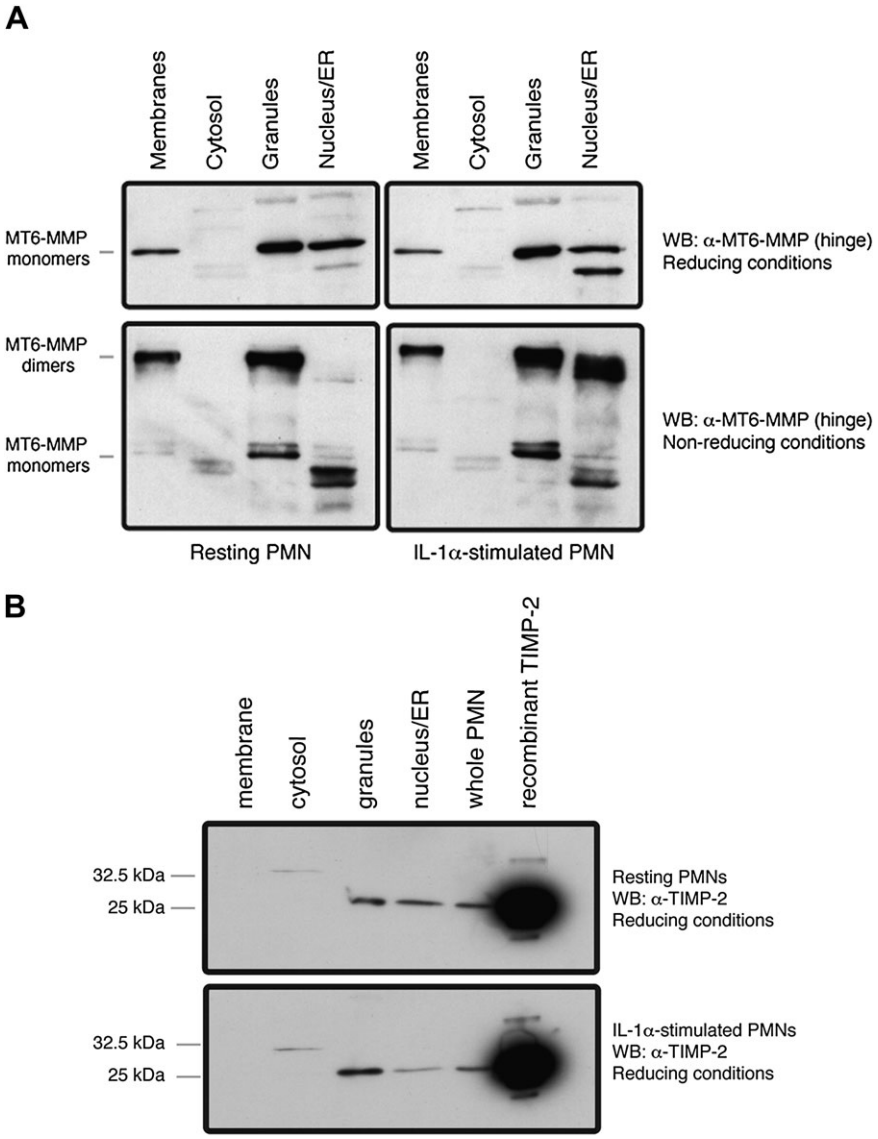

Fig. 1. Distribution of MT6-MMP and TIMP-2 in fractionated human PMNs. Freshly isolated PMNs (1×10^8 cells) were left untreated (resting) or were activated with IL-1α (100 U ml^{-1}) for 20 min at 37°C before being subjected to lysis by nitrogen cavitation. The cellular fractions were boiled in reducing or non-reducing (without β-ME) 2× sample buffer and resoled by SDS–PAGE followed by MT6-MMP detection (A). In (B), resting or activated PMNs were treated as described above but boiled in reducing sample buffer. The fractions were resolved by SDS–PAGE followed by TIMP-2 detection. These results were replicated in PMNs isolated from three independent blood donors.

stimulation with IL-1α, the relative level TIMP-2 in nuclear/ER/Golgi network fraction was significantly decreased ($P < 0.05$), suggesting a forward trafficking of TIMP-2 in response to IL-1α. Indeed, in IL-1α-stimulated PMNs, most of the TIMP-2 was found in granules (Fig. 1B, lower panel). Taken together, these results suggest that TIMP-2 shares a partial co-distribution with MT6-MMP in PMN granules and nuclear/ER fractions while PMN membranes are enriched with TIMP-2-free MT6-MMP dimers.

MT6-MMP is localized in lipid rafts of resting and stimulated human PMNs

MT6-MMP is a GPI-anchored MT-MMP that localizes in the lipid rafts (13, 15). Here we asked whether the lipid raft distribution of MT6-MMP is altered in resting and stimulated PMNs. To this end, membranes of resting and stimulated PMNs were isolated and subjected to sucrose gradient centrifugation, as described (20). Fractions were collected and subjected to immunoblot analyses for detection of MT6-MMP. These studies showed that monomeric and dimeric forms of MT6-MMP predominantly localize in lipid rafts (fractions # 1 and 2), as indicated by the co-localization of MT6-MMP with flotillin-1, a lipid raft marker (27) (Fig. 2A, uppermost and third panel). The presence of flottillin-1 in the raft fractions also confirmed the quality of the fractionation procedure. PMNs' stimulation with IL-1α had little effect on the distribution of MT6-MMP in the lipid rafts (Fig. 2A). As opposed to MT6-MMP, TIMP-2, a well-known inhibitor of MT6-MMP, was

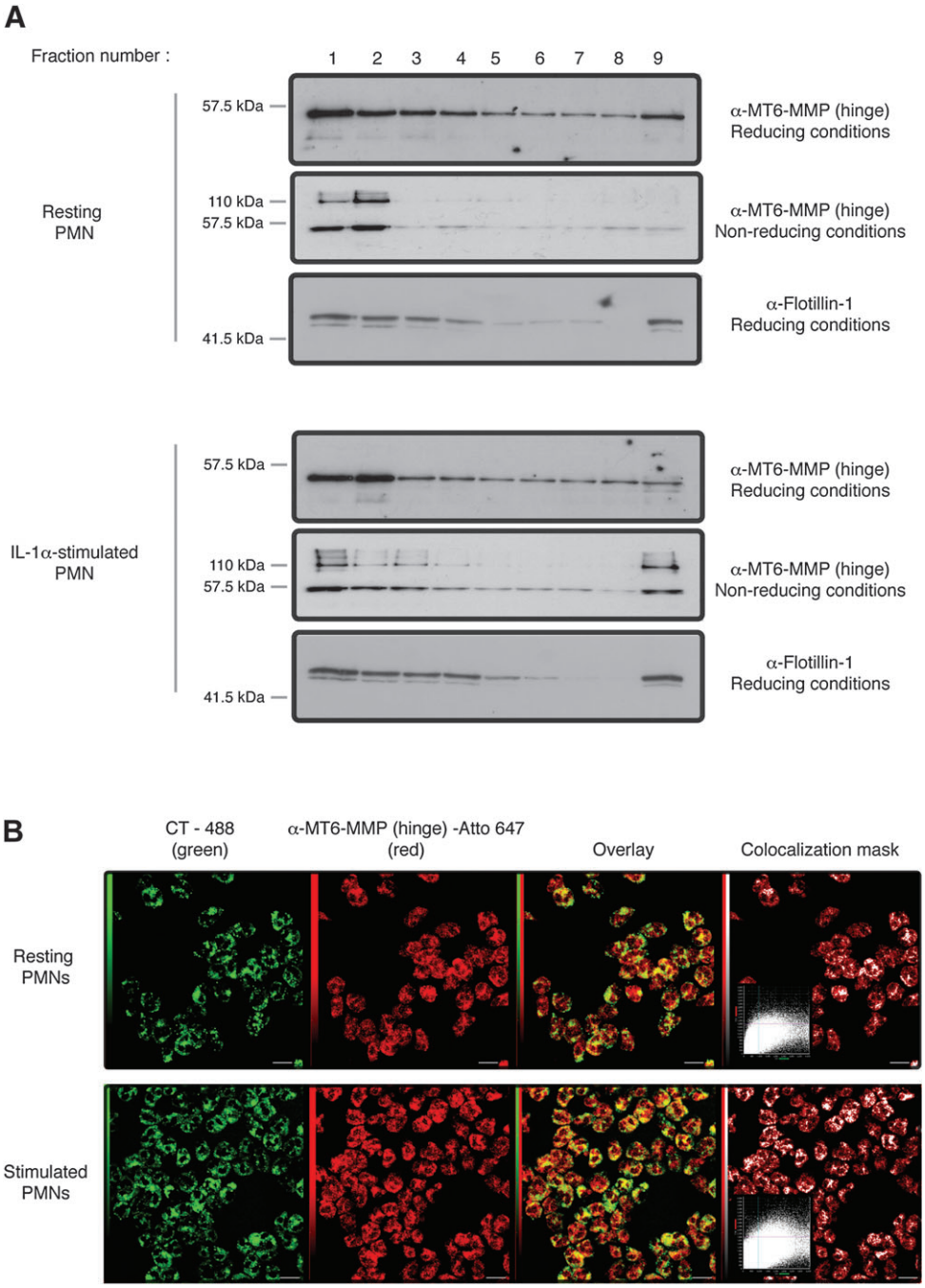

Fig. 2. MT6-MMP is localized in lipid rafts of resting and stimulated human PMNs. Freshly isolated PMNs were left untreated or were stimulated with IL-1α (100 U ml^{-1}) for 20 min at 37°C before processing for sucrose gradient fractionation (A) or confocal microscopy (B). In (A), PMN lysates (4×10^7 cells) were overlaid by a sucrose gradient and ultracentrifuged. Nine fractions were collected from the top of the gradient and boiled in reducing or non-reducing 2× sample buffer, as indicated, before MT6-MMP or flotillin-1 detection. (B) PMNs (1×10^6 cells) were fixed by PFA and permeabilized by 0.1% Triton X-100. The cells were then stained for lipid rafts with cholera toxin (CT-488) and the MT6-MMP hinge antibody, as described in Methods. Images were acquired by confocal microscopy, and co-localization between CT-488 and MT6-MMP is shown in the overlay as intense yellow pixels. These results are representative three independent blood donors.

not detected in both the raft and non-raft fractions (data not shown). This is consistent with our previous results of Fig. 1(B) where TIMP-2 was not detected in membranes in either resting or stimulated PMNs. The distribution of MT6-MMP in lipid rafts was also examined in thin cross sections of PMNs by confocal microscopy using fluorescently labeled cholera toxin, known to specifically bind to ganglioside GM1, which is present in lipid rafts (28). As shown in Fig. 2(B), MT6-MMP co-localizes with cholera toxin (Fig. 2B, overlay and co-localization mask, third and fourth panels, respectively),

further demonstrating that MT6-MMP is present in the lipid rafts, in agreement with our previous fractionation studies (Fig. 2A). Moreover, the quantification of co-localizing pixels with fluorograms (as described in Methods) revealed that ~91% of total MT6-MMP is localized in lipid rafts; stimulation with IL-1α did not significantly alter this distribution (94% after IL-α stimulation). Together, these results establish MT6-MMP as a component of PMN's lipid rafts and suggest that MT6-MMP is not displaced from the lipid rafts upon stimulation; to the contrary, TIMP-2 is excluded from the lipid rafts.

Human PMNs release MT6-MMP and stimulation increases its catalytic activity

Because the majority of MT6-MMP is localized intracellularly (11), we investigated the release of MT6-MMP from PMNs under resting or stimulated conditions. To this end, PMNs were left untreated or treated with a variety of stimuli, and cell-free supernatants were tested for MT6-MMP's presence by immunoprecipitation. We detected MT6-MMP in the supernatants of both resting and stimulated PMNs (Fig. 3A). We confirmed that PMA stimulation significantly increased MT6-MMP release by densitometric analysis (Fig. 3B), as previously reported (11). In contrast, stimulation with IFN-γ or other stimuli (LPS, TNF-α, IL-10, IL-18, fMLP or GM-CSF) did not significantly increase MT6-MMP release (Fig. 3A and B and data not shown). To insure the specificity of our immunoprecipitations, supernatants were incubated with normal rabbit IgG and/or beads only and tested for MT6-MMP's presence (Fig. 3C).

We next examined whether the released MT6-MMP exhibited catalytic activity against a general metalloproteinase peptide substrate. MT6-MMP released from unstimulated PMNs displayed a small catalytic activity (1.4-fold relative activity over control medium) (Fig. 3D), suggesting that the constitutively released MT6-MMP is active. Furthermore, MT6-MMP released from PMA- or IFN-γ-activated PMNs had a significantly increased catalytic activity compared with that of MT6-MMP released from unstimulated PMNs (Fig. 3D). In contrast, the catalytic activity of MT6-MMP released from fMLP-activated PMNs was not increased compared with that of unstimulated PMNs. We then tested if other stimuli (LPS, TNF-α, IL-18 or GM-CSF) could increase the catalytic activity of released MT6-MMP, but no increase in catalytic activity was found (data not shown). Taken together, these studies suggest that PMNs release catalytically active MT6-MMP and that some stimuli are able to directly, or indirectly, increase the catalytic activity of released MT6-MMP.

MT6-MMP faces inward in living human PMNs

Freshly purified, living human PMNs were examined for surface MT6-MMP expression by flow cytometry. To insure the detection of only living cells, PMNs were stained with PI, which specifically stains DNA and therefore indicate damaged or necrotic cells. These PI-positive cells were excluded from the analyses by appropriate gating. Interestingly, no signal for MT6-MMP was detected in living, non-permeabilized PMNs under these conditions (Fig. 4A). In contrast, living PMNs were strongly stained by the CD16 antibody, an Fcγ receptor present on the surface of PMNs (29) (Fig. 4A). Furthermore, living PMNs displayed no staining for IκB-α, a cytosolic protein that inhibits NF-κB activation (19) (data not shown). To verify if we could detect MT6-MMP intracellularly, PMNs were fixed and permeabilized before staining as described above. As shown in Fig. 4(B), a strong MT6-MMP staining was clearly detected under these conditions, consistent with the presence of intracellular MT6-MMP in PMNs. To further examine the surface localization of MT6-MMP, living PMNs were biotinylated and MT6-MMP was detected by SDS–PAGE as described under Methods. As shown in Fig. 4(C), this approach also failed to detect MT6-MMP at the surface of living PMNs, in agreement with our flow cytometry results (Fig. 4A). These results suggest that MT6-MMP is not present on the extracellular side of living PMNs.

MT6-MMP relocates to the cellular surface in apoptotic human PMNs

Park *et al.* (30) reported that apoptotic human PMNs display higher levels of MHC-II, CD80, CD86, CD83 and CD40 on the cell surface than freshly isolated cells. Since in living PMNs MT6-MMP is intracellularly distributed, we decided to test whether a fraction of the intracellular pool of MT6-MMP would relocate on the cell surface in apoptotic PMNs. To this end, we compared the surface expression of MT6-MMP in living and apoptotic PMNs by flow cytometry. As shown in Fig. 5(A), incubation of PMNs in RPMI for 24 h resulted in the occurrence of apoptosis, characterized by Annexin V and PI staining, for 60.7% of the cells. In contrast, exposure to GM-CSF reduced PMNs' apoptosis to 37.9% (Fig. 5A, left panel). Analyses of MT6-MMP expression under these conditions revealed that freshly isolated PMNs were negative for surface MT6-MMP (Fig. 5B, left panel), as shown in Fig. 4(A). In contrast, apoptotic PMNs, which stain for Annexin V and PI in Fig. 5(A), displayed MT6-MMP staining (Fig. 5B, middle panel). Addition of GM-CSF reduced the staining for MT6-MMP (Fig. 5B, right panel), consistent with its ability to reduce Annexin V and PI staining in Fig. 5(A). Analyses of permeabilized apoptotic and living PMNs showed similar levels of total MT6-MMP staining (Supplementary Figure 1 is available at *International Immunology* Online), indicating that the observed differences in MT6-MMP staining were not due to technical limitations. These results suggest that there is a differential distribution of MT6-MMP on the cellular surface between living and apoptotic PMNs.

Putative contribution of intracellular metalloproteinases to human PMN functions

The cellular location of MT6-MMP in living PMNs suggests that it could contribute to PMNs' cellular functions. Indeed, MT6-MMP is a membrane-bound, lipid raft-located enzyme and its catalytic domain can thus have access to the signaling machinery of PMNs. Testing this hypothesis in primary cells, however, requires the use of a selective MT6-MMP inhibitor, which is not yet available. We therefore decided to examine the role of metalloproteinase activity in PMN functions using GM6001, a broad-spectrum hydroxamate-type metalloproteinase inhibitor. GM6001 inhibits the activity of the recombinant catalytic domain of MT6-MMP (A. Sohal

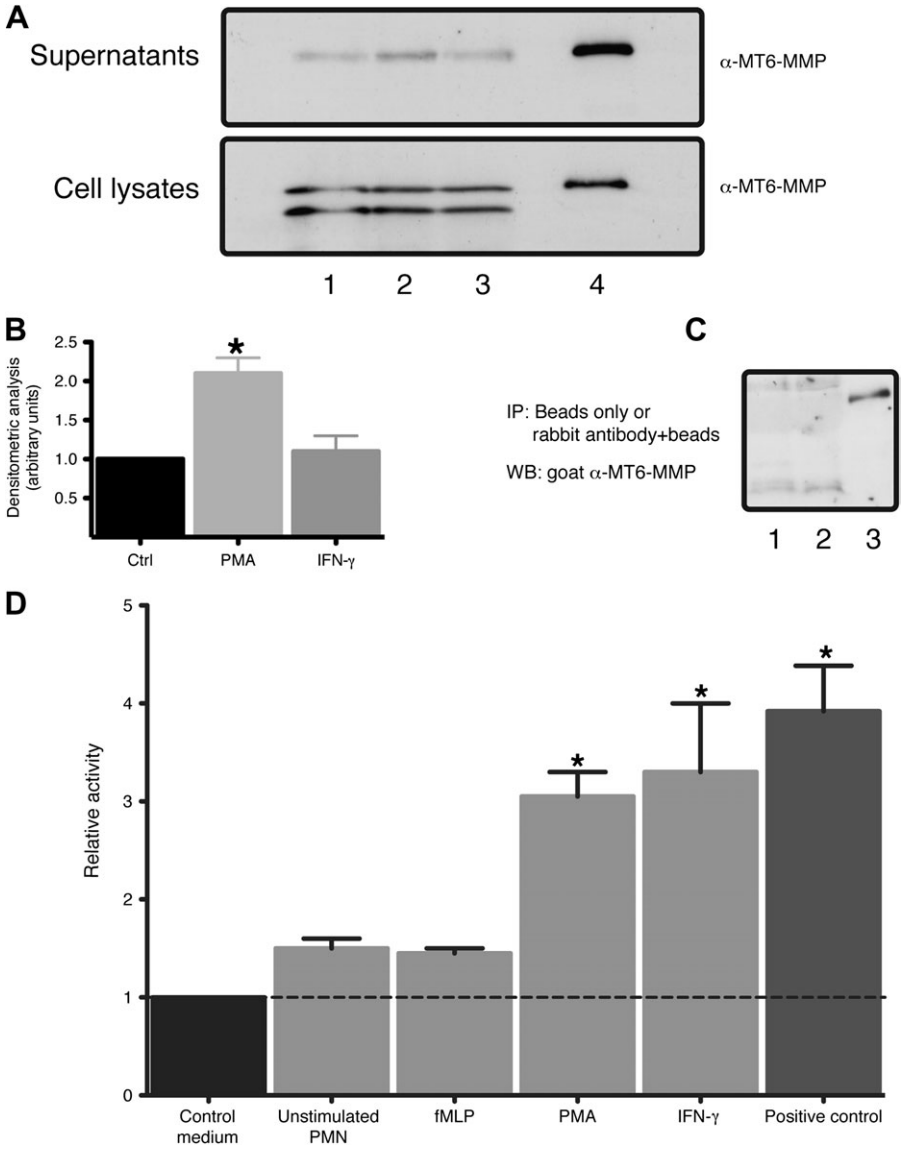

Fig. 3. MT6-MMP is released from human PMNs and is catalytically active. (A) PMNs (2×10^7 cells) were allowed to sediment for 55 min at 37°C before being left untreated (lane 1) or stimulated with 4 nM PMA (lane 2) or 100 U ml^{-1} IFN-γ (lane 3) for 20 min at 37°C. After stimulation, the media were centrifuged and both supernatants and cell pellets were collected for analysis. MT6-MMP was immunoprecipitated from the supernatants and the cell pellets were boiled in reducing 2× sample buffer. The immunoprecipitates and the cell lysates were resolved by SDS–PAGE, containing recombinant MT6-MMP (lane 4), followed by MT6-MMP detection. In (B), MT6-MMP was immunoprecipitated from the supernatants of resting or activated PMNs, resolved by SDS–PAGE and quantified by densitometry. These results are from three different blood donors and statistical significance is depicted as follows: $*P < 0.05$ compared with resting PMNs (Ctrl). (C) The specificity of the MT6-MMP immunoprecipitation was assessed as follows: supernatants were incubated with protein A/G beads alone (lane 1) or protein A/G beads and non-immune antibody (lane 2) and resolved by SDS–PAGE. Lane 3 shows recombinant MT6-MMP. (D) MT6-MMP was immunoprecipitated from supernatants of resting or stimulated PMNs (4 nM PMA, 100 U ml^{-1} IFN-γ or 30 nM fMLP for 20 min at 37°C). After several washes, the immunoprecipitates were incubated with a synthetic fluorescence-quenched peptide substrate for 5 h at room temperature. Hydrolysis of the fluorogenic substrate, representing MT6-MMP catalytic activity, was monitored with a spectrofluorometer. As negative control, the substrate was incubated with protein A/G beads and a control antibody (rabbit IgG), but with no PMNs (control medium). As a positive control, whole PMN lysates were incubated with the substrate as described above. The results are shown as mean relative activity ± SEM of three independent blood donors over control medium. Statistical significance is depicted as follows: $*P < 0.05$ compared with unstimulated PMNs.

and R. Fridman unpublished data) and of metalloproteinases from PMN lysates (Supplementary Figure 2 is available at *International Immunology* Online). We first examined the effect of GM6001 on respiratory burst by PMNs as the bactericidal activity of PMNs depends in part on their ability to generate superoxide species. We found that 5 μM GM6001 significantly decreased ($P < 0.01$) the respiratory burst, as measured by DCFDA cleavage, induced by PMA (Fig. 6A) or by fMLP (Fig. 6B). We also examined the effect of GM6001 on fMLP-induced chemotaxis of PMNs in Boyden chamber. These studies, however, showed that 5 μM GM6001 had no effect on PMN chemotaxis (data not

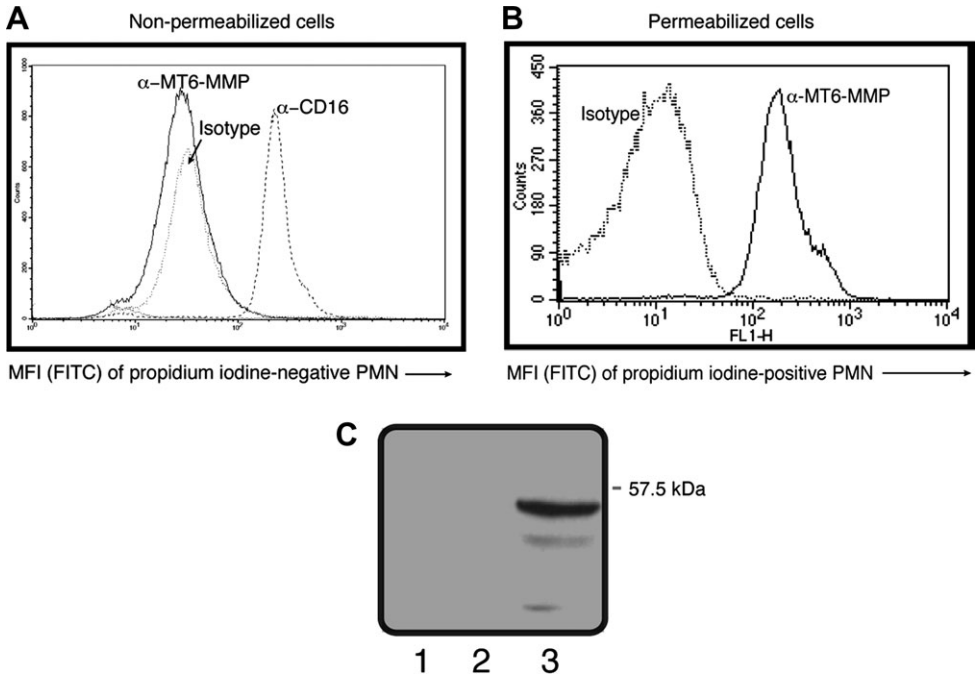

Fig. 4. MT6-MMP faces inward in human living PMNs. Freshly isolated PMNs (2.5×10^5 cells) were left untreated (non-permeabilized) (A) or were permeabilized by 0.1% Triton X-100 (B) and then stained with PI and antibodies against MT6-MMP hinge region or CD16 or with an appropriate isotype control. Resulting fluorescence was read by flow cytometry gating on PI-negative cells (non-permeabilized cells) or PI-positive cells (permeabilized cells). In (C), surface proteins of freshly isolated PMNs were biotinylated as described under Methods. Biotinylated proteins were then captured by avidin beads and subjected to reducing SDS–PAGE followed by MT6-MMP detection. Lane 1, non-biotinylated PMNs; lane 2, biotinylated PMNs and lane 3, recombinant MT6-MMP. Shown here are representative results that were replicated in three different blood donors.

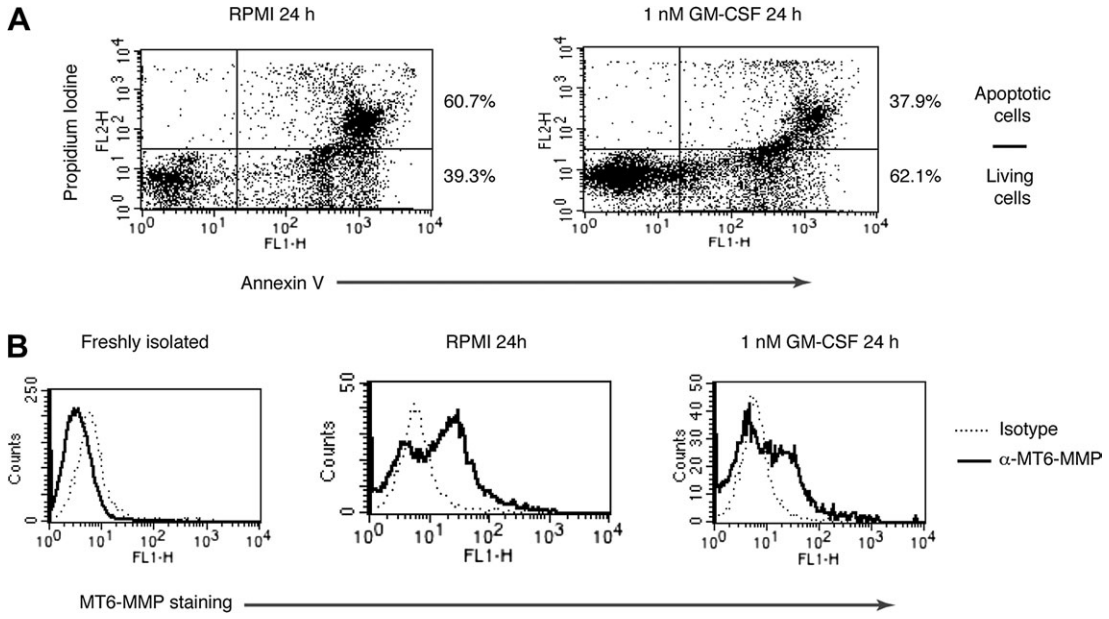

Fig. 5. Intracellular MT6-MMP relocates to the cell surface in apoptotic PMNs. PMNs (1×10^6 cells) were cultured in the absence (RPMI) or presence of 1 nM GM-CSF for 24 h at 37°C. Thereafter, PMNs were tested for apoptosis by PI and Annexin V staining without cell permeabilization (A). The percentages of living and apoptotic cells after the indicated treatment are shown on the right. (B) Cells in (A) were also stained with either an anti-MT6-MMP or control isotype antibody. These results were replicated in three different blood donors.

shown). Since PMNs are an important source of secreted cytokines during the immune response (5, 6), we studied the effect of GM6001 on LPS- and TNF-α-induced PMN secretion of IL-8 by PMNs. As shown in Fig. 7, the addition of 5 μM GM6001 before stimulation significantly decreased the release of IL-8 in response to both LPS and TNF-α. As the

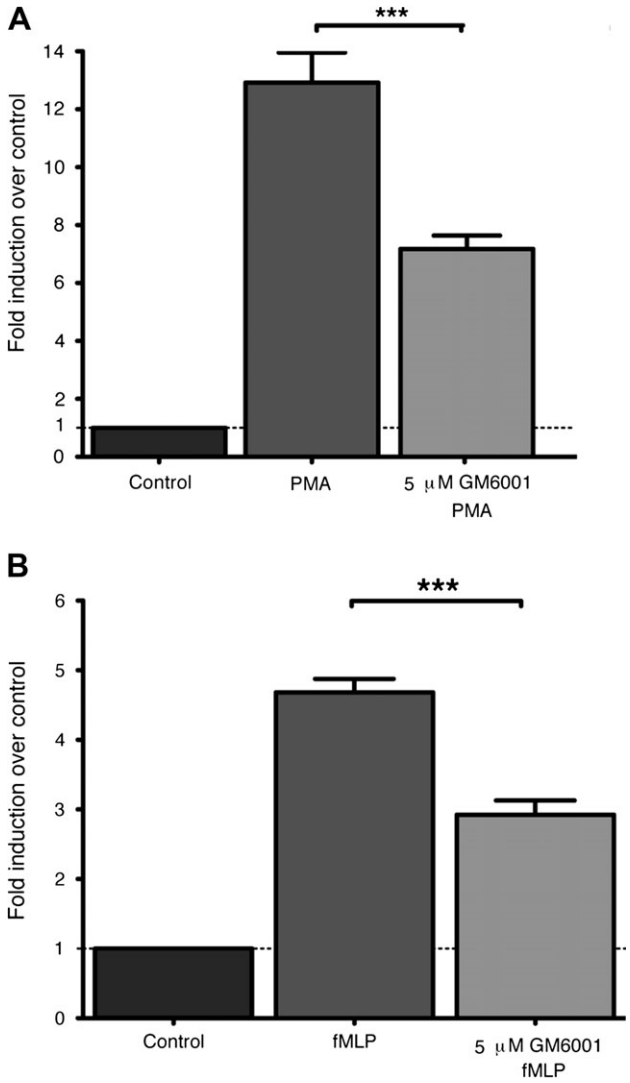

Fig. 6. Metalloproteinase activity is involved in PMN respiratory burst. PMNs (1×10^6) were loaded with 20 μM DCFDA and stimulated with 4 nM PMA (A) or 30 nM fMLP (B) for 10 min at 37°C. Fluorescence was then read by flow cytometry and the data are presented as a stimulation index ± SEM computed as follows: MFI of activated cells relative to MFI of resting cells but loaded with DCFDA (Control). Where indicated, 5 μM GM6001 was incubated for 30 min at 37°C with PMNs before DCFDA loading and stimulation. The results shown are from a compilation of three independent blood donors. Statistical significance is depicted as follows: ***$P < 0.01$.

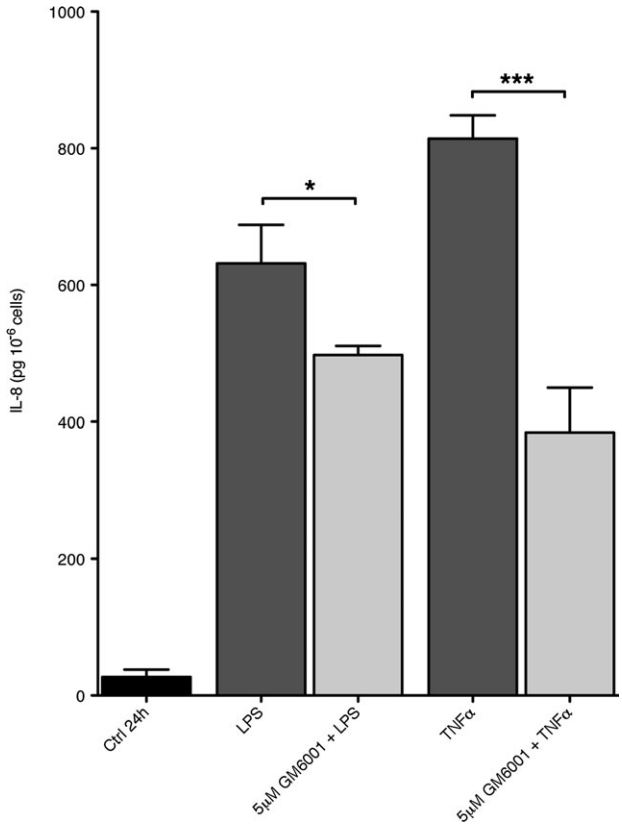

Fig. 7. Metalloproteinase activity contributes to chemokine release by stimulated PMNs. PMNs (3×10^6) were cultured in 24-well plates at 37°C for 24 h in the presence or absence (Ctrl) of LPS (100 ng ml^{-1}) or TNF-α (100 U ml^{-1}) in RPMI. Where indicated, GM6001 was added before the stimulation. And, measurement of secreted IL-8 in supernatants was done by ELISA. The results are shown as mean IL-8 ± SEM (pg 10^{-6} cells) from a compilation of three independent blood donors. The statistical significance is depicted as follows: *$P < 0.05$, ***$P < 0.01$.

apoptosis of effector cells is important for the resolution of inflammation, we tested whether PMNs' lifespan would be influenced by GM6001. PMNs cultured 24 h with GM-CSF could be rescued from apoptosis, as determined by Annexin V and PI staining; however, the addition of 5 μM GM6001 had no effect on the GM-CSF-induced PMNs' survival (Supplementary Figure 3 is available at *International Immunology* Online; compare panel B to panel C). We observed, however, that 5 μM GM6001 increased the rate of spontaneous apoptosis (Supplementary Figure 3 is available at *International Immunology* Online; compare panel A with panel E). Collectively, these results suggest that metalloproteinase activity contributes to PMN functions, such as respiratory burst and chemokine secretion.

Discussion

MT6-MMP, a GPI-anchored metalloproteinase, was described previously as highly expressed in PMNs and distributed in the granules and in the plasma membrane (11). Our data presented herein confirm and extend the previously described cell distribution of MT6-MMP in human PMNs: the protease is present in the granules and the nuclear/ER fraction, and a minor fraction is retained in membranes even upon stimulation. Moreover, MT6-MMP is detected as a high molecular weight form of 120 kDa representing disulfide-bonded homodimers of active protease (14), indicating that this form is the natural organization of MT6-MMP in PMNs. In addition, a minor 45-kDa immunoreactive form is detected in the nuclear/ER fraction after stimulation in non-reducing conditions. This minor immunoreactive form possibly represents a degradation product and/or an underglycosylated precursor species of MT6-MMP in this particular fraction. Here we also report that as a GPI-containing protein,

MT6-MMP distributes into the lipid raft fraction co-localizing with specific raft markers. This is in agreement with an early proteomic analysis study in bovine PMNs that identified MT6-MMP as a component of lipid rafts using mass spectrometry (15). We found that lipid rafts of PMNs contain both the homodimeric and the monomeric form of MT6-MMP, indicating that dimerization is not a prerequisite for insertion into PMN's lipid rafts. Indeed, dimerization-defective mutants of MT6-MMP were shown to distribute into lipid rafts like the wild-type protease (14). Functionally, lipid rafts are required for PMNs to efficiently fulfill their inflammatory duties, such as superoxide production (31, 32) and phagocytosis (33–35). Our data suggest that lipid rafts could serve to concentrate MT6-MMP activity in a defined cellular compartment, possibly to target specific components thereof. Alternatively, MT6-MMP could associate with receptors whose recruitment to lipid rafts were described in PMNs, such as BLT-1 (leukotriene B4 receptor) (27), FcγRIIIb (36), Toll-like receptors-2/4 (37) and triggering receptor expressed on myeloid cells-1 (21). However, the putative substrates of MT6-MMP in lipid rafts remain to be identified.

The activity of metalloproteinases, including MT6-MMP, is controlled by TIMPs, which specifically interact with the catalytic site hence inhibiting proteolysis. We previously demonstrated that the catalytic activity of membrane-anchored MT6-MMP is inhibited by both TIMP-1 and TIMP-2 (24). Here our data show that, in human PMNs, MT6-MMP exhibits a partial co-distribution with TIMP-2 in the granules and in the nuclear/ER fraction. In contrast, TIMP-2 was excluded from lipid rafts, possibly due to its soluble nature and/or due to dissociation from MT6-MMP during lipid raft preparation or its transport to the lipid rafts via the Trans Golgi Network, although our data cannot distinguish between these possibilities. The total absence of TIMP-2 in lipid rafts suggests that a significant pool of active MT6-MMP in PMNs is TIMP free and thus capable of unregulated proteolysis. This suggestion, however, cannot be construed as a lack of sensitivity to TIMP inhibition by MT6-MMP in lipid rafts since exogenously administered TIMPs inhibit catalytic activity of membrane-anchored MT6-MMP, as we demonstrated with isolated plasma membranes of cells expressing recombinant MT6-MMP (24).

Consistent with the presence of MT6-MMP in PMN gelatinase granules and secretory vesicles (11), we found that MT6-MMP was released into the supernatant of PMNs in a constitutive manner and was catalytically active. Because of the cultured conditions used here, the constitutive release of active MT6-MMP from PMNs is likely to require β2-integrin engagement and adherence. These conditions, β_2-integrin engagement and adherence, were found to enhance TNF-α signaling (38) and induce MMP-9 secretion in PMNs (39). Indeed, we found that culture conditions that do not induce β2-integrin engagement (when cellular density is lower than 20×10^7 cells per ml in culture) did not result in MT6-MMP release, as measured by immunoprecipitation, in resting or stimulated PMNs (data not shown). The release of MT6-MMP under conditions involving integrin engagement together with the reported ability of MT6-MMP to cleave extracellular matrix components (24) suggest a potential role for MT6-MMP in the transit of human PMNs through the endothelium during inflammation.

Further research is needed to further characterize protein interactions of native MT6-MMP and to explore the regulation of its enzymatic activity. Recent findings, for example indicate that clusterin, an abundant serum protein, can form complexes with MT6-MMP and inhibits its enzymatic activity (16). It is thus possible that some specific stimuli can induce the dissociation of clusterin–MT6-MMP complexes, leading to MT6-MMP activation but that other stimuli cannot induce their dissociation and, therefore, cannot induce MT6-MMP activation. This could explain the differences observed herein between IFN-γ and fMLP; both did not induce additional MT6-MMP secretion but IFN-γ induced MT6-MMP activity, whereas fMLP did not. These also suggest that the induction of MT6-MMP activity may be partly the result of an indirect activation resulting from IFN-γ-induced signaling pathways.

PMNs are inherently short-lived cells and consequently undergo a defined program of apoptosis that helps to remove aged and dysfunctional PMNs to terminate the inflammatory response in sites of infection. The apoptotic program of PMNs is characterized by specific morphological and molecular changes including the differential expression of surface molecules (40). In our experimental settings, we found that freshly isolated, living PMNs do not display MT6-MMP on the cellular surface. Conversely, we found that apoptotic PMNs displayed high levels of MT6-MMP on the cell surface. Moreover, rescuing PMNs from apoptosis with GM-CSF reduced the level of MT6-MMP on the cellular surface. MT6-MMP, however, was readily detected in permeabilized living or apoptotic PMNs, suggesting that these results were not caused by technical limitations. Our results, however, cannot help to specify from which cellular compartment the re-distributed MT6-MMP in apoptotic PMNs originates. Furthermore, the eventual targets of a possible MT6-MMP activity on the surface of apoptotic PMNs, if MT6-MMP is active in this context, are still unknown. However, although not shown in this study, we can rule out pro-MMP-9 as a substrate of MT6-MMP on the cellular surface of apoptotic PMNs because MT6-MMP is not an activator of pro-MMP-9, as previously shown (13). It is conceivable that MT6-MMP contributes to the shedding or processing of surface molecules that modulate the resolution of apoptosis by efferocytosis.

To probe the potential contribution of MT6-MMP in human PMN functions, we used a broad-spectrum metalloproteinase inhibitor, GM6001, because a specific MT6-MMP inhibitor is not available yet. Our studies indicate a differential effect of GM6001 in key PMN activities *in vitro*, which provide indirect evidence on the relative contribution of metalloproteinase activity in some PMN functions, such as Reactive Oxygen Species production and chemokine generation. Conversely, metalloproteinases are not required for the motile response of PMNs induced by fMLP because GM6001 had no effect on fMLP-induced chemotaxis. This result is consistent with a number of previous *in vitro* studies showing the lack of effect of MMP inhibitors on fMLP-stimulated chemotaxis or migration across endothelial cells of PMNs and on Tsup-1, a T-cell line, chemotaxis (41, 42).

In summary, in living (resting and stimulated) PMNs, the majority of MT6-MMP is present in intracellular granules and membranes. The membrane-anchored TIMP-2-free MT6-MMP is present as monomeric and dimeric disulfide-bonded forms that are localized within the lipid rafts but are not displayed on the cellular surface. In living PMNs, membrane-anchored MT6-MMP may contribute to cytokine secretion and respiratory burst. During apoptosis, membrane-anchored MT6-MMP becomes externalized and is readily displayed on the surface of PMNs. Active MT6-MMP is constitutively released from intracellular stores in resting PMNs; however, certain stimuli may induce further release of intracellular MT6-MMP. The validation of our findings with GM6001 awaits the development of specific MT6-MMP inhibitors and the results of ongoing studies using mice deficient in MT6-MMP; but taken together, our results provide new insights on the role of MT6-MMP in the physiology of human PMNs.

Supplementary data

Supplementary data are available at *International Immunology* Online.

Funding

NCI-NIH (CA61986 to R.F.); Canadian Institutes of Health Research (No 63149 to T.F.); Research Center on Aging of the Sherbrooke Geriatric University Institute.

Acknowledgements

C.F.F. is the recipient of a studentship from the Canadian Institutes of Health Research. The authors are greatly indebted to Leonid Volkov for the help in confocal microscopy. Authorship: C.F.F., A.S. and Q.S. performed the experiments and wrote the first draft of the manuscript. R.F., T.F. and C.F.F. designed the study and, with P.P.M., wrote the final version of the manuscript.

References

1 Serhan, C. N. and Savill, J. 2005. Resolution of inflammation: the beginning programs the end. *Nat. Immunol.* 6:1191.
2 Ren, Y., Xie, Y., Jiang, G. *et al.* 2008. Apoptotic cells protect mice against lipopolysaccharide-induced shock. *J. Immunol.* 180:4978.
3 Maslinska, D. and Gajewski, M. 1998. Some aspects of the inflammatory process. *Folia Neuropathol.* 36:199.
4 Nathan, C. 2006. Neutrophils and immunity: challenges and opportunities. *Nat. Rev. Immunol.* 6:173.
5 Scapini, P., Lapinet-Vera, J. A., Gasperini, S., Calzetti, F., Bazzoni, F. and Cassatella, M. A. 2000. The neutrophil as a cellular source of chemokines. *Immunol. Rev.* 177:195.
6 Kasama, T., Miwa, Y., Isozaki, T., Odai, T., Adachi, M. and Kunkel, S. L. 2005. Neutrophil-derived cytokines: potential therapeutic targets in inflammation. *Curr. Drug Targets Inflamm. Allergy* 4:273.
7 Scapini, P., Carletto, A., Nardelli, B. *et al.* 2005. Proinflammatory mediators elicit secretion of the intracellular B-lymphocyte stimulator pool (BLyS) that is stored in activated neutrophils: implications for inflammatory diseases. *Blood* 105:830.
8 Borregaard, N., Sorensen, O. E. and Theilgaard-Monch, K. 2007. Neutrophil granules: a library of innate immunity proteins. *Trends Immunol.* 28:340.
9 Opdenakker, G., Van den Steen, P. E., Dubois, B. *et al.* 2001. Gelatinase B functions as regulator and effector in leukocyte biology. *J. Leukoc. Biol.* 69:851.
10 Van Lint, P. and Libert, C. 2006. Matrix metalloproteinase-8: cleavage can be decisive. *Cytokine Growth Factor Rev.* 17:217.
11 Kang, T., Yi, J., Guo, A. *et al.* 2001. Subcellular distribution and cytokine- and chemokine-regulated secretion of leukolysin/MT6-MMP/MMP-25 in neutrophils. *J. Biol. Chem.* 276:21960.
12 Pei, D. 1999. Leukolysin/MMP25/MT6-MMP: a novel matrix metalloproteinase specifically expressed in the leukocyte lineage. *Cell Res.* 9:291.
13 Sun, Q., Weber, C. R., Sohail, A. *et al.* 2007. MMP25 (MT6-MMP) is highly expressed in human colon cancer, promotes tumor growth, and exhibits unique biochemical properties. *J. Biol. Chem.* 282:21998.
14 Zhao, H., Sohail, A., Sun, Q. *et al.* 2008. Identification and role of the homodimerization interface of the glycosylphosphatidylinositol-anchored membrane type 6 matrix metalloproteinase (MMP25). *J. Biol. Chem.* 283:35023.
15 Nebl, T., Pestonjamasp, K. N., Leszyk, J. D., Crowley, J. L., Oh, S. W. and Luna, E. J. 2002. Proteomic analysis of a detergent-resistant membrane skeleton from neutrophil plasma membranes. *J. Biol. Chem.* 277:43399.
16 Matsuda, A., Itoh, Y., Koshikawa, N., Akizawa, T., Yana, I. and Seiki, M. 2003. Clusterin, an abundant serum factor, is a possible negative regulator of MT6-MMP/MMP-25 produced by neutrophils. *J. Biol. Chem.* 278:36350.
17 Nie, J. and Pei, D. 2004. Rapid inactivation of alpha-1-proteinase inhibitor by neutrophil specific leukolysin/membrane-type matrix metalloproteinase 6. *Exp. Cell Res.* 296:145.
18 Boyum, A. 1968. Isolation of mononuclear cells and granulocytes from human blood. Isolation of mononuclear cells by one centrifugation, and of granulocytes by combining centrifugation and sedimentation at 1 g. *Scand. J. Clin. Lab. Invest.* 97 (Suppl.):77.
19 Ear, T., Cloutier, A. and McDonald, P. P. 2005. Constitutive nuclear expression of the I kappa B kinase complex and its activation in human neutrophils. *J. Immunol.* 175:1834.
20 Fortin, C. F., Larbi, A., Lesur, O., Douziech, N. and Fulop, T. Jr. 2006. Impairment of SHP-1 down-regulation in the lipid rafts of human neutrophils under GM-CSF stimulation contributes to their age-related, altered functions. *J. Leukoc. Biol.* 79:1061.
21 Fortin, C. F., Lesur, O. and Fulop, T. Jr. 2007. Effects of TREM-1 activation in human neutrophils: activation of signaling pathways, recruitment into lipid rafts and association with TLR4. *Int. Immunol.* 19:41.
22 Laemmli, U. K. 1970. Cleavage of structural proteins during the assembly of the head of bacteriophage T4. *Nature* 227:680.
23 English, W. R., Velasco, G., Stracke, J. O., Knauper, V. and Murphy, G. 2001. Catalytic activities of membrane-type 6 matrix metalloproteinase (MMP25). *FEBS Lett.* 491:137.
24 Sohail, A., Sun, Q., Zhao, H., Bernardo, M. M., Cho, J. A. and Fridman, R. 2008. MT4-(MMP17) and MT6-MMP (MMP25), a unique set of membrane-anchored matrix metalloproteinases: properties and expression in cancer. *Cancer Metastasis Rev.* 27:289.
25 Opdenakker, G., Masure, S., Grillet, B. and Van Damme, J. 1991. Cytokine-mediated regulation of human leukocyte gelatinases and role in arthritis. *Lymphokine Cytokine Res.* 10:317.
26 Masure, S., Proost, P., Van Damme, J. and Opdenakker, G. 1991. Purification and identification of 91-kDa neutrophil gelatinase. Release by the activating peptide interleukin-8. *Eur. J. Biochem.* 198:391.
27 Sitrin, R. G., Emery, S. L., Sassanella, T. M., Blackwood, R. A. and Petty, H. R. 2006. Selective localization of recognition complexes for leukotriene B4 and formyl-Met-Leu-Phe within lipid raft microdomains of human polymorphonuclear neutrophils. *J. Immunol.* 177:8177.
28 Blank, N., Schiller, M., Krienke, S., Wabnitz, G., Ho, A. D. and Lorenz, H. M. 2007. Cholera toxin binds to lipid rafts but has a limited specificity for ganglioside GM1. *Immunol. Cell Biol.* 85:378.
29 Fernandez-Segura, E., Garcia, J. M., Lopez-Escamez, J. A. and Campos, A. 1994. Surface expression and distribution of Fc receptor III (CD16 molecule) on human natural killer cells and polymorphonuclear neutrophils. *Microsc. Res. Tech.* 28:277.
30 Park, H. Y., Jin, J. O., Song, M. G., Park, J. I. and Kwak, J. Y. 2007. Expression of dendritic cell markers on cultured neutrophils and

its modulation by anti-apoptotic and pro-apoptotic compounds. *Exp. Mol. Med.* 39:439.
31 Shao, D., Segal, A. W. and Dekker, L. V. 2003. Lipid rafts determine efficiency of NADPH oxidase activation in neutrophils. *FEBS Lett.* 550:101.
32 Otabor, I., Tyagi, S., Beurskens, F. J. *et al.* 2004. A role for lipid rafts in C1q-triggered O_2^- generation by human neutrophils. *Mol. Immunol.* 41:185.
33 Yanagida, M., Nakayama, H., Yoshizaki, F. *et al.* 2007. Proteomic analysis of plasma membrane lipid rafts of HL-60 cells. *Proteomics* 7:2398.
34 Yoshizaki, F., Nakayama, H., Iwahara, C., Takamori, K., Ogawa, H. and Iwabuchi, K. 2008. Role of glycosphingolipid-enriched microdomains in innate immunity: microdomain-dependent phagocytic cell functions. *Biochim. Biophys. Acta* 1780:383.
35 Nakayama, H., Yoshizaki, F., Prinetti, A. *et al.* 2008. Lyn-coupled LacCer-enriched lipid rafts are required for CD11b/CD18-mediated neutrophil phagocytosis of nonopsonized microorganisms. *J. Leukoc. Biol.* 83:728.
36 David, A., Fridlich, R. and Aviram, I. 2005. The presence of membrane proteinase 3 in neutrophil lipid rafts and its colocalization with FcgammaRIIIb and cytochrome b558. *Exp. Cell Res.* 308:156.
37 Fulop, T., Larbi, A., Douziech, N. *et al.* 2004. Signal transduction and functional changes in neutrophils with aging. *Aging Cell.* 3:217.
38 Avdi, N. J., Nick, J. A., Whitlock, B. B. *et al.* 2001. Tumor necrosis factor-alpha activation of the c-Jun N-terminal kinase pathway in human neutrophils. Integrin involvement in a pathway leading from cytoplasmic tyrosine kinases apoptosis. *J. Biol. Chem.* 276:2189.
39 Wize, J., Sopata, I., Smerdel, A. and Maslinski, S. 1998. Ligation of selectin L and integrin CD11b/CD18 (Mac-1) induces release of gelatinase B (MMP-9) from human neutrophils. *Inflamm. Res.* 47:325.
40 Kennedy, A. D. and DeLeo, F. R. 2009. Neutrophil apoptosis and the resolution of infection. *Immunol. Res.* 43:25.
41 Xia, M., Leppert, D., Hauser, S. L. *et al.* 1996. Stimulus specificity of matrix metalloproteinase dependence of human T cell migration through a model basement membrane. *J. Immunol.* 156:160.
42 Mackarel, A. J., Cottell, D. C., Russell, K. J., FitzGerald, M. X. and O'Connor, C. M. 1999. Migration of neutrophils across human pulmonary endothelial cells is not blocked by matrix metalloproteinase or serine protease inhibitors. *Am. J. Respir. Cell Mol. Biol.* 20:1209.